Lymphomagenic CARD11/BCL10/MALT1 signaling drives malignant B-cell proliferation via cooperative NF-κB and JNK activation

Nathalie Knies[a], Begüm Alankus[a], Andre Weilemann[b,c], Alexandar Tzankov[d], Kristina Brunner[a], Tanja Ruff[a], Marcus Kremer[e], Ulrich B. Keller[f], Georg Lenz[b,c], and Jürgen Ruland[a,g,h,1]

[a]Institut für Klinische Chemie und Pathobiochemie, Klinikum Rechts der Isar, Technische Universität München, 81675 Munich, Germany; [b]Translational Oncology, Department of Medicine A, University Hospital Münster, 48149 Münster, Germany; [c]Cells in Motion, Cluster of Excellence EXC 1003, 48149 Münster, Germany; [d]Institute of Pathology, University Hospital Basel, 4031 Basel, Switzerland; [e]Institut für Pathologie, Klinikum Harlaching, 81545 Munich, Germany; [f]Department of Medicine III, Klinikum Rechts der Isar, Technische Universität München, 81675 Munich, Germany; [g]German Cancer Consortium, 69120 Heidelberg, Germany; and [h]German Center for Infection Research, 81675 München, Germany

The aggressive activated B cell-like subtype of diffuse large B-cell lymphoma is characterized by aberrant B-cell receptor (BCR) signaling and constitutive nuclear factor kappa-B (NF-κB) activation, which is required for tumor cell survival. BCR-induced NF-κB activation requires caspase recruitment domain-containing protein 11 (CARD11), and CARD11 gain-of-function mutations are recurrently detected in human diffuse large B-cell lymphoma (DLBCL). To investigate the consequences of dysregulated CARD11 signaling in vivo, we generated mice that conditionally express the human DLBCL-derived CARD11 (L225LI) mutant. Surprisingly, CARD11(L225LI) was sufficient to trigger aggressive B-cell lymphoproliferation, leading to early postnatal lethality. CARD11(L225LI) constitutively associated with B-cell CLL/lymphoma 10 (BCL10) and mucosa-associated lymphoid tissue lymphoma translocation gene 1 (MALT1) to simultaneously activate the NF-κB and c-Jun N-terminal kinase (JNK) signaling cascades. Genetic deficiencies of either BCL10 or MALT1 completely rescued the phenotype, and pharmacological inhibition of JNK was, similar to NF-κB blockage, toxic to autonomously proliferating CARD11(L225LI)-expressing B cells. Moreover, constitutive JNK activity was observed in primary human activated B cell-like (ABC)-DLBCL specimens, and human ABC-DLBCL cells were also sensitive to JNK inhibitors. Thus, our results demonstrate that enforced activation of CARD11/BCL10/MALT1 signaling is sufficient to drive transformed B-cell expansion in vivo and identify the JNK pathway as a therapeutic target for ABC-DLBCL.

diffuse large B-cell lymphoma | CARD11 | NF-κB | JNK | mouse model

Diffuse large B-cell lymphoma (DLBCL) is the most frequent lymphoma in adults. It is an aggressive disease that comprises several subsets, including the activated B cell-like (ABC) and germinal-center B cell-like (GCB) subtypes (1); the ABC subset in particular is characterized by poor survival (2). ABC-DLBCL cells exhibit gene expression signatures similar to normal B cells activated by B-cell receptor (BCR) engagement and a constitutive activation of the canonical nuclear factor kappa-B (NF-κB) pathway, which is essential for survival of the tumor cells (3, 4). Canonical NF-κB signaling is regulated by IκB kinase β (IKKβ), which induces proteolytic degradation of inhibitory IκB proteins by their phosphorylation and thereby allows translocation of NF-κB transcription factors into the nucleus. Although small molecule inhibitors of IKKβ efficiently block the growth of ABC-DLBCL cells in vitro (5), clinical trials failed due to highly toxic side effects (NCT00003979) (6, 7).

Physiological NF-κB activation by the BCR is initiated by receptor-proximal tyrosine kinases, such as spleen tyrosine kinase (SYK) and Bruton agammaglobulinemia tyrosine kinase (BTK), which trigger activation of downstream modules, including protein kinase C, beta-1 (PKCβ) and phosphatidylinositol 3-kinase

(PI3K) (reviewed in ref. 8). The key link to the IKK complex is the scaffolding molecule caspase recruitment domain-containing protein 11 (CARD11), which is inactive in resting cells due to an intramolecular inhibitory interaction between its linker region and its coiled-coil domain (9). B-cell activation induces PKCβ-mediated phosphorylation of CARD11, which relieves the protein from autoinhibition, resulting in recruitment of the adapter protein B-cell CLL/lymphoma 10 (BCL10) and paracaspase mucosa-associated lymphoid tissue lymphoma translocation gene 1 (MALT1), and the formation of the CARD11/BCL10/MALT1 (CBM) complex. Further recruitment of activating factors such as TRAF proteins and casein kinase 1 α (CK1α), as well as IKKs and TAK1, leads to IKK and c-Jun N-terminal kinase (JNK) activation (10, 11).

RNA interference screens have revealed that CARD11, BCL10, and MALT1 are all essential for survival of ABC-DLBCL cells, consistent with the key role of the CBM complex in NF-κB activation (12). Moreover, a series of gain-of-function mutations that disrupt the autoinhibitory mechanism were identified in the coiled-coil domain of CARD11 in human DLBCL (13). Regardless, the

Significance

The activated B cell-like (ABC) subtype of diffuse large B-cell lymphoma (DLBCL) has a poor clinical outcome and is characterized by constitutive caspase recruitment domain-containing protein 11 (CARD11)/B-cell CLL/lymphoma 10 (BCL10)/mucosa-associated lymphoid tissue lymphoma translocation gene 1 (MALT1) signaling and nuclear factor kappa-B (NF-κB) activation, which is essential for tumor cell survival. However, NF-κB inhibitors have not reached the clinic due to high toxicity, and alternative strategies for targeted therapies are needed. Using mouse genetics, we demonstrate that forced CARD11/BCL10/MALT1 signaling drives lethal lymphoproliferation through simultaneous NF-κB and c-Jun N-terminal kinase (JNK) activation. Pharmacological inhibition of JNK was similar to NF-κB blockage and toxic to autonomously proliferating murine B cells, and constitutive JNK activity was observed in human ABC-DLBCL cells, which are also sensitive to JNK inhibitors. Our results identify the JNK pathway as a therapeutic target for DLBCL.

consequences of constitutive activation of CARD11 signaling in normal B cells remain unclear, and the downstream effectors that mediate the aberrant CARD11 activity remain to be identified.

Here, we generated a mouse model for conditional expression of a human DLBCL-derived CARD11(L225LI) gain-of-function mutant and demonstrated that CARD11(L225LI) autonomously associates with BCL10 and MALT1 and cooperatively activates NF-κB and JNK signaling, resulting in a rapidly lethal lymphoproliferative disorder. Moreover, we observed constitutive JNK activation in primary human ABC-DLBCL specimens and showed that JNK inhibition was toxic to murine CARD11(L225LI)-expressing B cells and human ABC-DLBCL lymphoma cells. Our data demonstrate that the forced activation of CBM signaling is sufficient to drive lethal lymphoproliferation in vivo and highlight JNK as a potential target for the treatment of ABC-DLBCL patients.

Results

CARD11(L225LI) Expression in B Cells Drives a Rapidly Lethal Lymphoproliferative Disease.

To investigate constitutive active CARD11 signaling, we first introduced the human lymphoma-derived CARD11(L225LI) mutant into the mature B-cell lymphoma line Bal-17 and studied B-cell activation in vitro (Fig. S1). Compared with cells transfected with WT CARD11, CARD11(L225LI)-expressing cells exhibited strong up-regulation of the activation marker CD80 and down-regulation of IgM, indicating B-cell activation (Fig. S1A). A gel mobility shift assay demonstrated that CARD11(L225LI) expression resulted in robust induction of NF-κB DNA-binding activity that could be enhanced by BCR simu-

lation (Fig. S1B). These results are in accordance with published data (14) and demonstrate that forced expression of CARD11 (L225LI) is sufficient to induce constitutive NF-κB signaling and to trigger B-cell activation. Because the CARD11(L225LI) mutant induces stronger NF-κB activation than other patient-derived or artificially generated CARD11 gain-of-function variants (13, 14), we used CARD11(L225LI) to study enforced CARD11 signaling in vivo. To this end, we introduced a human *Card11(L225LI)* cDNA fused to a hemagglutinin (HA) tag preceded by a loxP-flanked (FL) transcriptional and translational STOP cassette into the mouse genome at the ubiquitously expressed *ROSA26* locus (Fig. S2) (15). Crossing CARD11 (L225LI)^{stopFL} mice with CD19-Cre transgenic animals (16) resulted in excision of the loxP-flanked STOP cassette specifically in the B-cell lineage as early as the pre–B-cell stage. Subsequent bicistronic expression of CARD11(L225LI), together with enhanced green fluorescent protein (eGFP), allowed fluorescence monitoring of the CARD11(L225LI)-expressing cells. For simplicity, we refer to the CD19-Cre and CARD11(L225LI)^{stopFL} double transgenic mice throughout this study as CARD11 (L225LI)$^{CD19-Cre}$ mice.

Strikingly, all of the CARD11(L225LI)$^{CD19-Cre}$ mice died within 6 d of birth (Fig. 1A), with massive splenomegaly and lymphadenopathies resulting from dramatic increases in the frequency and total number of CD19-expressing, GFP-positive B lymphocytes (Fig. 1 B–D). Histological examination of the transgenic spleens showed homogenous populations of large cells with prominent nucleoli and high proliferation indices (>75%), as assayed by Ki-67 staining (Fig. 1E). These blastoid cells infiltrated solid organs,
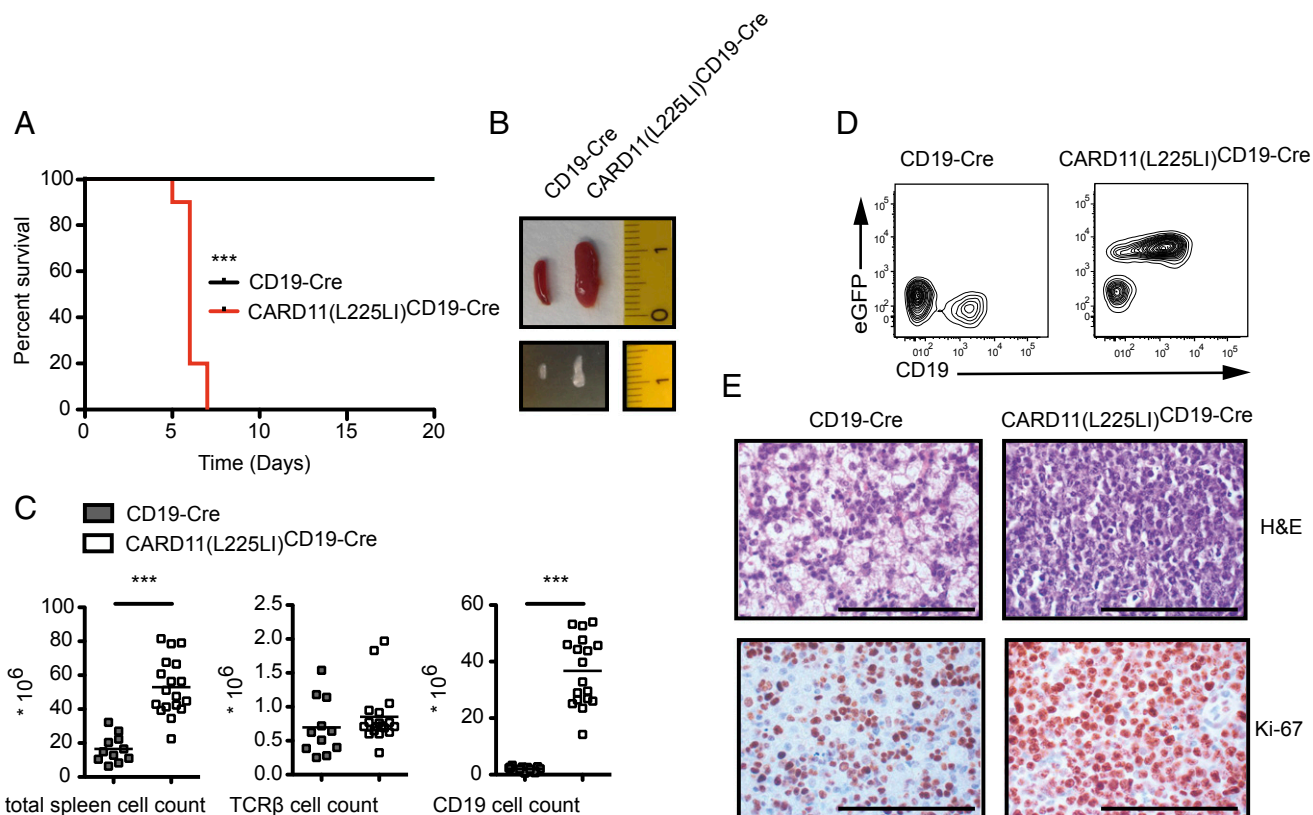
Fig. 1. CARD11(L225LI) drives lethal lymphoproliferation in vivo. (A) Kaplan–Meier curve of CD19-Cre and CARD11(L225LI)$^{CD19-Cre}$ mice (n = 15 each). (B) Macroscopic appearance of representative spleens and mesenteric lymph nodes (in cm). (C) Total counts of splenocytes and TCRβ- or CD19-expressing cells; bars indicate mean. (D) Representative frequencies of CD19- and eGFP-expressing cells in the splenic lymphocyte gate. (E) Disruption of the splenic architecture, with highly proliferative cells in the CARD11(L225LI)$^{CD19-Cre}$ mice, was revealed by H&E staining and immunohistochemistry using anti-Ki-67 antibodies (representative of three mice of each genotype). (Scale bars: 1 mm.) The data shown in B–E are obtained from 5-d-old animals.

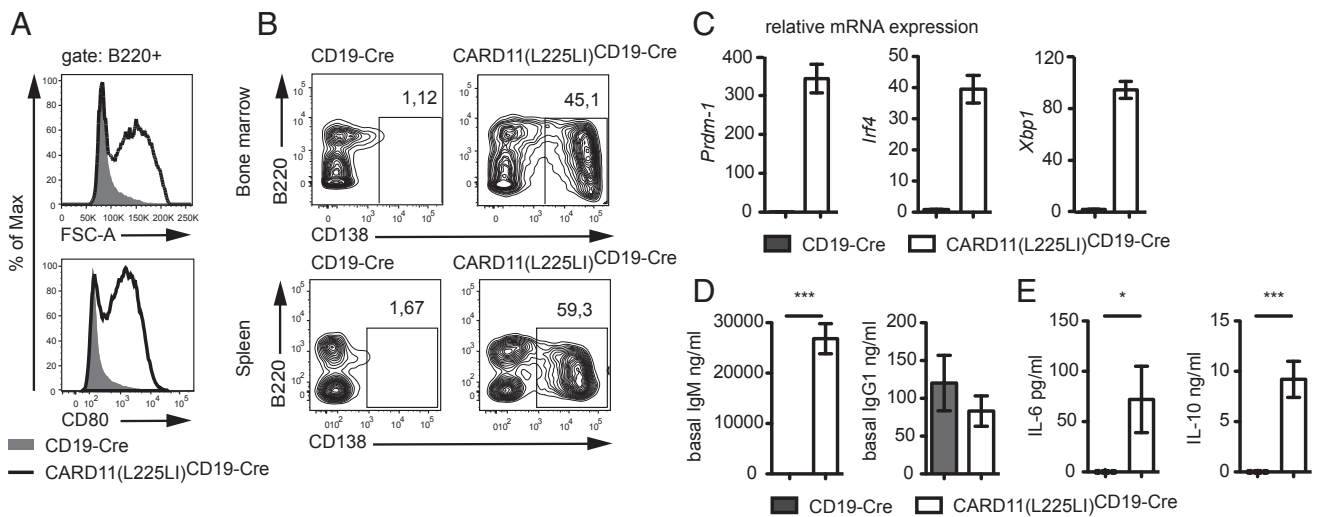**Fig. 2.** CARD11(L225LI) leads to dysregulated B-cell differentiation. (*A*) CARD11(L225LI)-expressing B cells show an activated phenotype in vivo: forward-scatter area (FSC-A) and CD80 expression were measured using flow cytometry. (*B*) Representative analysis of B-cell populations within bone marrow (BM) and spleens of 5-d-old animals by flow cytometry. The numbers refer to the mean percentages of B cells in the total BM-nucleated cells and splenocytes; cells were pregated for the lymphocyte population. The data shown in *A* and *B* are representative of six independent experiments, with a total number of at least 11 mice analyzed per genotype. (*C*) Transcript levels of *Prdm-1*, *Irf4*, and *Xbp1* in MACS-purified CD19-Cre and CARD11(L225LI)$^{CD19-Cre}$ B cells, normalized to *Hprt1*; $n \geq 4$ per genotype. (*D*) Basal serum IgG1 ($n \geq 8$ mice per genotype) and IgM ($n = 11$ mice per genotype). (*E*) Sera from ≥ 20 animals per genotype were analyzed using the Th1/Th2 FlowCytomix kit. The data are shown as the mean $\pm$ SEM.

including the liver, thus displaying the characteristic histopathological features of high-grade lymphoma. Detailed flow cytometric analysis of B-cell development revealed that the CARD11(L225LI)-expressing cells exhibited an activated phenotype with high CD80 and Sca-1 expression and elevated CD43 levels, together with an increased forward-scatter (FSC) due to the large cell size (Fig. 2*A* and Fig. S3 *A* and *B*). The B220$^+$IgM$^-$ compartment in the bone marrow was massively reduced compared with WT, indicating bone marrow infiltration by peripheral blastoid B cells. These cells express only low levels of the IL-7 receptor or CD25, demonstrating that the disease does not resemble acute B-cell lineage leukemia (Fig. S3 *C* and *D*). The CARD11(L225LI)-expressing B cells in the bone marrow and spleen of the CARD11(L225LI)$^{CD19-Cre}$ animals were CD138-positive, and they exhibited low B220 expression, indicating that they consisted of plasmablasts (B220^{int}CD138$^+$) and plasma cells (B220^{low}CD138$^+$) (Fig. 2*B*). Consistently, they did not express CD21 or the κ-light chain but were IgMI^{ow}, MHCII^{low} and CXCR4$^+$ (Fig. S3 *E–G*) (17). To further characterize the B-cell differentiation phenotype of these transgenic cells, we performed RT-PCR analysis of *Prdm-1, Irf4*, and *Xbp1* expression. These markers of plasma cell differentiation were highly expressed in the CARD11(L225LI)-expressing B cells (Fig. 2*C*).

To test whether these plasmablastic B cells produced antibodies, we analyzed sera for the presence of IgM and class-switched IgG1 (Fig. 2*D*). Although we found comparable concentrations of IgG1 in both genotypes, we observed strongly increased concentrations of IgM in the sera of the CARD11(L225LI)$^{CD19-Cre}$ mice as well as high concentrations of IL-6 and IL-10, cytokines that are also autonomously produced by ABC-DLBCL cells (Fig. 2*E*) (18). Together, these findings reveal that the selective expression of CARD11(L225LI) in otherwise unmanipulated B lymphocytes is sufficient to drive B cells into dysregulated plasmablastic differentiation and massive proliferation, resulting in a highly aggressive lymphomatous disease that leads to early lethality with 100% penetrance.

CARD11(L225LI)-Induced Lymphoproliferation Is Strictly Dependent on BCL10 and MALT1. As indicated above, under physiological conditions, WT CARD11 associates in a BCR signal-dependent

manner with BCL10 and MALT1 to mediate B-cell activation (4). To obtain insight into the effectors of pathological CARD11 (L225LI) signaling, we tested whether CARD11(L225LI) also engaged CBM complexes. To this end, we immunoprecipitated the CBM-associated kinase CK1α (1, 19) from acutely explanted CARD11(L225LI) transgenic or WT B cells and tested associations with CARD11, BCL10, and MALT1 by Western blots. CBM complexes were constitutively assembled in the CARD11 (L225LI) transgenic B cells, but not in resting control B lymphocytes (Fig. 3*A*). We next investigated whether formation of BCL10- and MALT1-containing complexes is causative for lethal CARD11(L225LI)-mediated lymphoproliferation by crossing CARD11(L225LI)$^{CD19-Cre}$ transgenic mice into BCL10- or MALT1-deficient backgrounds [CARD11(L225LI)$^{CD19-Cre}$; BCL10$^{-/-}$ or CARD11(L225LI)$^{CD19-Cre}$;MALT1$^{-/-}$] (2, 20, 21). Intriguingly, the deficiency of either BCL10 or MALT1 completely rescued the CARD11(L225LI)$^{CD19-Cre}$ mice from early lethality (Fig. 3*B*). Moreover, the CARD11(L225LI)$^{CD19-Cre}$;BCL10$^{-/-}$ or CARD11(L225LI)$^{CD19-Cre}$;MALT1$^{-/-}$ B lymphocytes were not enlarged and displayed no up-regulation of activation markers (Fig. 3 *C–E*). Thus, the constitutive assembly of CARD11(L225LI)-induced CBM complexes is solely responsible for the pathological B-cell activation, differentiation, and malignant proliferation.

CARD11(L225LI) Simultaneously Activates NF-κB and JNK Signaling. Because physiological CARD11/BCL10/MALT1 complexes mediate both BCR-induced NF-κB and JNK activation (4, 22), we speculated that the CARD11(L225LI) mutant could also simultaneously trigger the NF-κB and JNK pathways. To test this hypothesis, we performed Western blot analyses of cytosolic extracts from freshly isolated CARD11(L225LI)-expressing B lymphoblasts. Consistent with the activation of the IKK/NF-κB pathway, IκBα was constitutively phosphorylated in the CARD11(L225LI)-expressing B cells. Moreover, constitutive JNK activation was detected with activation state-specific anti-phospho-JNK antibodies. In agreement with these results, c-Jun, a key target transcription factor of JNK, was also detected at high levels in the CARD11(L225LI)-expressing cells (5, 23) (Fig. 4*A*).
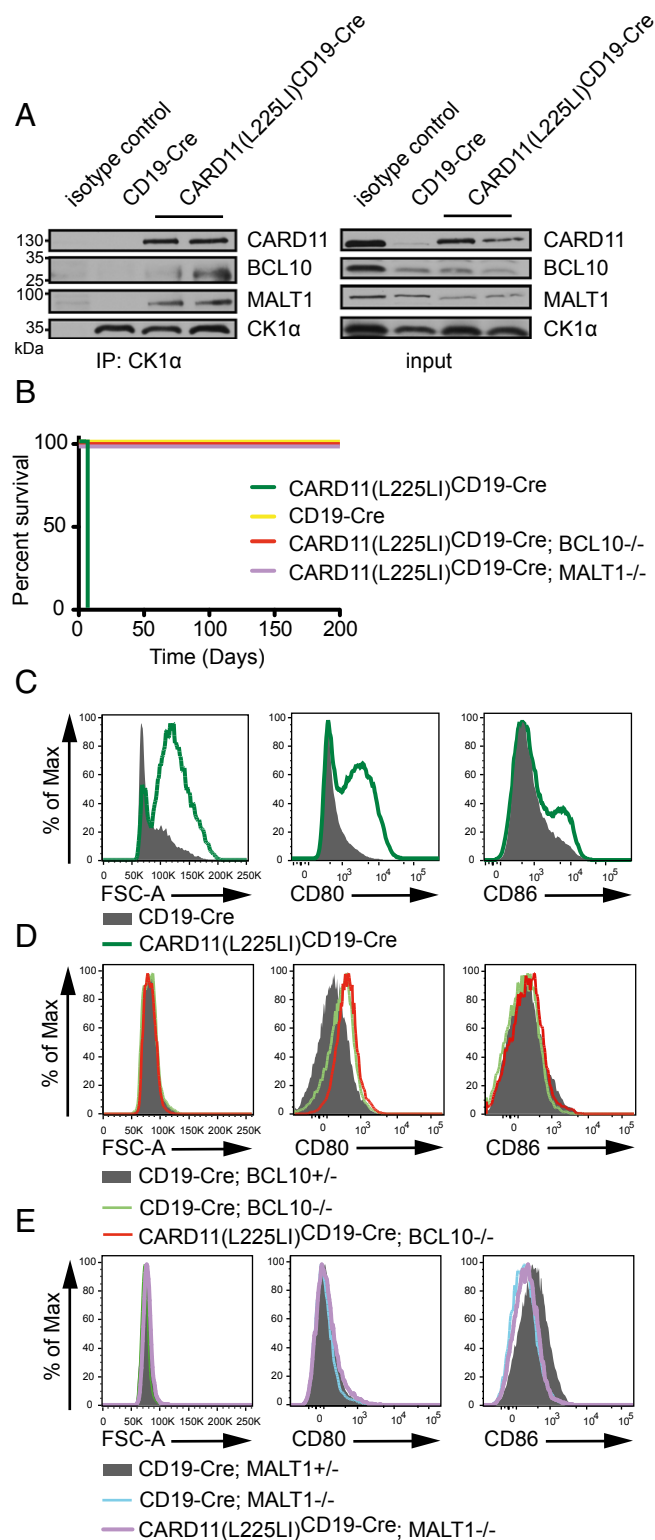
Fig. 3. CARD11(L225LI)-mediated B-cell activation strictly depends on BCL10 and MALT1. (A) Anti-CK1α immunoprecipitation using lysates from B lymphocytes of 5-d-old animals. (B) Kaplan–Meier curves of mice of indicated genotypes (each genotype, n ≥ 5). (C) Histogram of splenic B cells from 5-d-old CD19-Cre and CARD11(L225LI)^CD19-Cre mice. (D) Histogram of splenic B cells from 2- to 3-mo-old CD19-Cre;BCL10^+/−, CD19-Cre;BCL10^−/−, and CARD11 (L225LI)^CD19-Cre;BCL10^−/− mice. (E) CD19-Cre;MALT1^+/−, CD19-Cre;MALT1^−/−, and CARD11(L225LI)^CD19-Cre;MALT1^−/− mice. In C–E, expression of activation markers was assessed by flow cytometry; the analysis was performed in three independent experiments; n ≥ 4 per genotype.

We then performed cell fractionation to examine nuclear events. In CARD11(L225LI)-expressing B cells, we detected high nuclear levels of the NF-κB subunits RelA, cRel, and p50, a result congruent with constitutive active IKK signaling (Fig. 4B). In addition, and consistent with activated JNK signaling, we also observed high concentrations of the phosphorylated forms of the AP-1 transcription factors subunits c-Jun and Atf2 (6, 7, 24) in the nuclear extracts of CARD11(L225LI)-transgenic cells (Fig. 4C). Furthermore, transfection of CARD11(L225LI) into the Bal-17 cells in vitro also induced increased nuclear levels of RelA, cRel, and p50, as well as c-Jun (Fig. 4D). Moreover, gel mobility shift assays using nuclear extracts from acutely explanted CARD11(L225LI)-transgenic murine B cells demonstrated strongly enhanced NF-κB and AP-1 DNA binding activity in comparison with WT (Fig. 4E). Because neither constitutive NF-κB signaling nor constitutive JNK signaling was observed in the CARD11(L225LI)-expressing B cells that genetically lack either BCL10 or MALT1, we conclude that the CARD11(L225LI) mutant activates both IKK and JNK through a strictly BCL10- and MALT1-dependent manner (Fig. 4 F and G).

Constitutive JNK and NF-κB Signaling Is Essential for CARD11(L255LI)-Transgenic B-Cell Growth. To test whether activation of both NF-κB and JNK signaling is required for malignant expansion of CARD11 (L225LI)-expressing B lymphocytes and to study whether pharmacological inhibition of either cascade affects lymphoblast growth, we cultured primary CARD11(L225LI)-expressing B lymphocytes in vitro. In contrast to WT B cells, CARD11(L225LI)-transgenic lymphocytes survived and, indeed, proliferated vigorously, without the addition of any specific B-cell survival or mitogenic factor for at least 10 d in culture (Fig. 5A).

To inhibit IKK, we incubated the cells with the well-characterized synthetic inhibitor Bay11-7082 (8, 25). For JNK blockage, we treated lymphocytes with SP600125, which inhibits JNK, showing minimal off-target effects on MKK4 and MKK6 (9, 26); a derivate was clinically developed for idiopathic pulmonary fibrosis (NCT01203943), for which constitutive JNK activation has been shown (10, 11, 27, 28). We also incubated the transgenic B cells with small molecule compounds that inhibit SYK (R406) (NCT01499303) or BTK (PCI-32765; Ibrutinib) (NCT01325701) receptor-proximal tyrosine kinases or PI3K signaling (Cal-101, Idelalisib) (NCT01282424) and that are in clinical trials or approved for lymphoma therapy (12, 29, 30), or with the ERK inhibitor PD98,059. As expected, IKK inhibition resulted in strong reduction of nuclear NF-κB RelA, cRel, and p50, and inhibition of JNK activity blocked the presence of phosphorylated c-Jun and reduced the levels of phosphorylated Atf2 in the nucleus (Fig. 5 B and C). Moreover, the inhibition of neither SYK (R406) (Fig. 5D), BTK (Fig. 5E), PI3K (Fig. 5F), nor ERK (Fig. 5G) significantly affected viability or proliferation of CARD11(L225LI)-expressing B cells in culture, indicating that only the active CBM complex is required for their survival. Moreover, the responsiveness of the BCR is defective in CARD11 (L225LI)-expressing B cells because IgM cross-linking does not activate the proximal kinases (Fig. S4). In contrast to proximal kinase inhibition, the blockage of NF-κB signaling induced death in CARD11(L225LI)-expressing B cells, consistent with the sensitivity of human ABC-DLBCL cells to IKK inhibition (Fig. 5H). Moreover, pharmacological inhibition of JNK signaling with SP600125 also triggered death of CARD11(L225LI)-expressing cells (Fig. 5I), demonstrating that the pathological growth of CARD11(L225LI)-expressing B cells not only is dependent on dysregulated NF-κB signaling, but also critically requires JNK kinase activity. The on-target effects of the Bay11-7082 and SP600125 inhibitors are underscored by the fact that low doses of the compounds that do not kill CARD11(L225LI)-expressing B cells also do not affect p50 and phospho-c-Jun levels (Fig. S5).
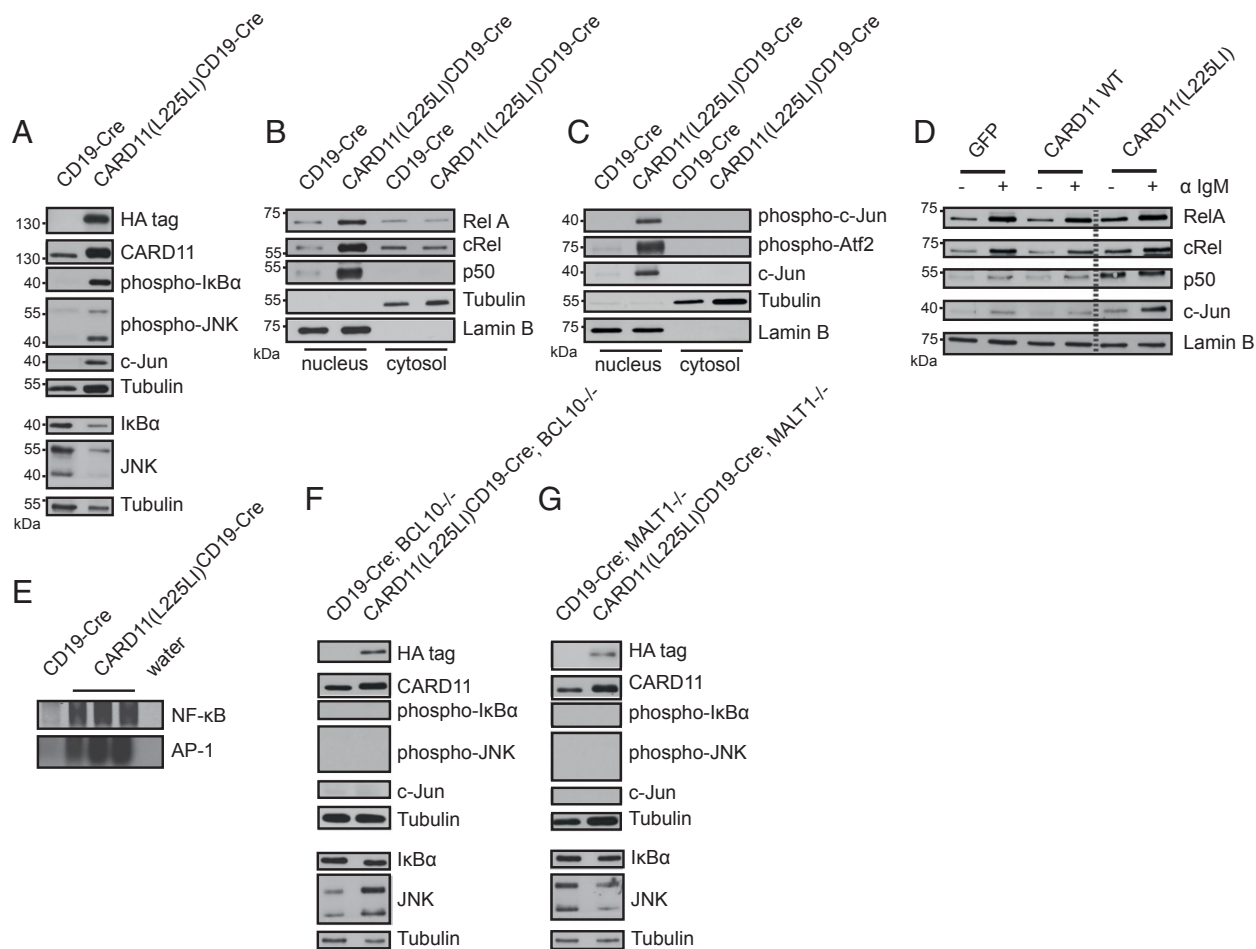
Fig. 4. AP-1 and NF-κB activation depends on CBM formation in CARD11(L225LI)-expressing cells. (*A*) Immunoblots of MACS-purified splenic B cells from indicated genotypes (5-d-old mice). Nuclear translocation of (*B*) NF-κB subunits and (*C*) AP-1 transcription factor subunits was assayed by immunoblotting. (*D*) Nuclear extracts from FACS-sorted GFP-positive retrovirally transduced Bal-17 cells expressing GFP or CARD11 WT and CARD11(L225LI) together with GFP were analyzed by Western blot. The data shown are representative of at least two independent experiments. (*E*) Nuclear extracts were subjected to a gel mobility shift assay for NF-κB and AP-1 DNA-binding activity. (*E–G*) Immunoblots of MACS-purified splenic B cells from indicated genotypes (6- to 12-wk-old mice). All lysates in *A–C* and *E–G* were obtained from at least three independent experiments of individual mice, and B cells from CD19-Cre mice were pooled in at least three independent experiments.

Human ABC-DLBCL Exhibits Constitutive JNK Activity. Based on our results in the genetically defined mouse model, we subsequently investigated the activity of JNK kinase in human DLBCL by immunohistochemistry analysis of primary specimens from 67 DLBCL patients for the presence of activated JNK. The DLBCL cases were categorized by their cell-of-origin subtypes according to the Tally algorithm (13, 31), revealing 47 non-GCB (ABC)-DLBCL and 20 GCB-DLBCL cases. Strikingly, none of the examined GCB-DLBCL samples (though single internal positive control nuclei were observable in the respective examined tissues), but more than 55% of the ABC-DLBCL biopsies, stained positive for phosphorylated JNK (Fig. 6*A*), demonstrating constitutive activation of JNK selectively in an ABC-DLBCL fraction. To study the functional role of JNK signaling in human DLBCL, we used a set of phenotypically well-characterized human ABC-DLBCL cell lines (HBL-1, OCI-Ly3, OCI-Ly10, and TMD8) (13, 14, 18). Interestingly, we also observed constitutive JNK phosphorylation in three of four ABC-DLBCL lines (Fig. 6*B*), and in vitro kinase assays with c-Jun as a substrate further confirmed constitutive JNK activity in these DLBCL cells (Fig. 6*C*). Thereafter, we transduced the non–ABC-type lymphoma cell line BJAB, which does not exhibit NF-κB or JNK activation, with the constitutive active CARD11 version alone or fused to GFP. The

activating CARD11 mutation resulted in activation of NF-κB, as defined by the presence of RelA, cRel, and p50 in the nucleus, and in JNK activation, as shown by Western blotting with anti–phospho-JNK antibodies (Fig. 6*D*) or JNK kinase assays, indicating that constitutively active CARD11 is sufficient to engage JNK in human lymphoma cells (Fig. 6*E*). Finally, we treated the human ABC-DLBCL cells with the JNK inhibitor SP600125 to investigate the relevance of the JNK pathway for survival of human ABC-DLBCL cells. Intriguingly, SP600125 mediated dose-dependent cell killing in the ABC-DLBCL cell lines HBL-1, OCI-Ly3, and OCI-Ly10 tumor cell lines with constitutive JNK activation. In contrast, TMD8 does not exhibit constitutive JNK activation. Thus, JNK inhibition is lethal for ABC-DLBCL cells with constitutive JNK activity, and these effects of SP600125 are unlikely due to nonspecific toxicity (Fig. 6*E*).

Discussion

Our analysis of a genetically defined mouse model of constitutively active CARD11 signaling and parallel investigations in human lymphoma demonstrates that aberrant CBM signaling is sufficient to drive lethal lymphoproliferation in vivo and identifies the JNK pathway as a key downstream effector essential for transformed B-cell growth.
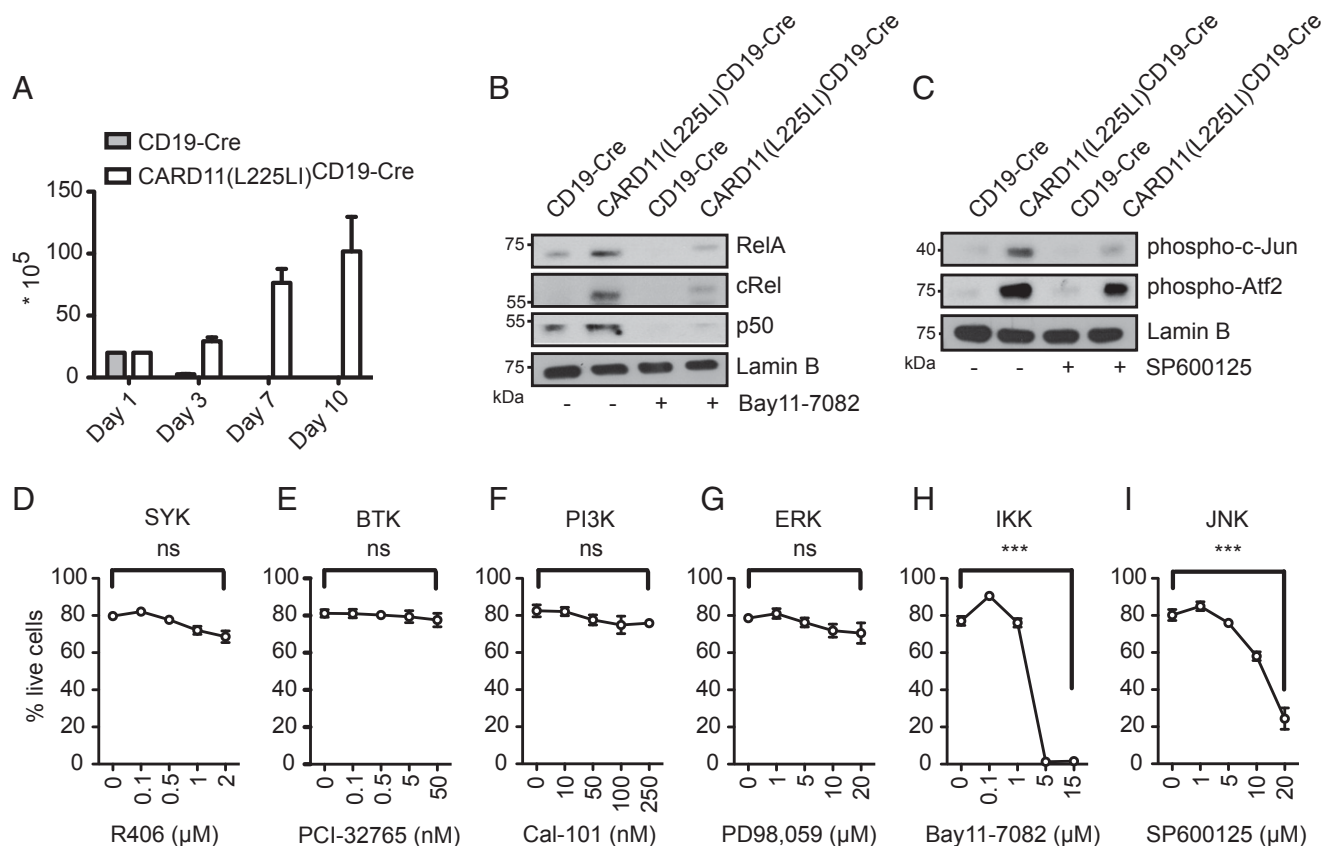
Fig. 5. CARD11(L225LI)-transformed cells are sensitive to inhibition of NF-κB or JNK signaling. (*A*) Survival and proliferation of CD19-Cre and CARD11(L225LI)$^{CD19-Cre}$ splenocytes was evaluated by a Trypan Blue exclusion assay. The experiment was conducted twice, with a total *n* = 7. CD19-Cre MACS-purified B cells and CARD11(L225LI)$^{CD19-Cre}$ splenocytes were treated with solvent control DMSO and (*B*) treated with 10 μM Bay11-7082 and (*C*) with 20 μM SP600125 for 4 h, and nuclear lysates were examined for the presence of (*B*) NF-κB subunits and (*C*) AP-1 subunits. Representative results from six experiments are shown. (*D–I*) Cells were cultured with solvent control DMSO or in the presence of the indicated inhibitors and concentrations for 48 h. Annexin V- and 7AAD-double-negative cells were determined cytometrically. The experiment was performed at least twice, with *n* ≥ 4. The data are presented as the mean ± SEM.

The malignant disease induced by CARD11(L225LI) expression in otherwise unmanipulated B cells develops very rapidly and results in lethality in all transgenic animals as early as 1 wk after birth. These surprising findings indicate that secondary mutations within the transgenic B cells or external triggers are probably not required to induce the aggressive disease. Crosses of CARD11(L225LI)$^{CD19-Cre}$ mice to BCL10- or MALT1-deficient animals completely rescued the phenotype, thereby excluding the possibility that lymphoma-derived CARD11 mutations could engage BCL10- or MALT1-independent pathways to drive pathogenesis. Moreover, our experiments with small molecule inhibitors against SYK, BTK, and PI3K revealed that autonomous growth of the transformed B cells is not affected by BCR proximal kinase blockage. Thus, aberrant CBM activity is, per se, oncogenic and independent from upstream input. These findings imply that human lymphomas with constitutive active CARD11 mutations might also not be sensitive to SYK, BTK, or PI3K inhibitors, which needs to be systematically investigated. Indeed, recent clinical data demonstrate that ABC-DLBCL tumors with CARD11 mutations do not respond to BTK inhibition with Ibrutinib (32).

One key downstream pathway that emerges from CBM complexes is the NF-κB signaling cascade. NF-κB is essential for ABC-DLBCL survival (12-14, 33), and IKK inhibition is toxic for CARD11(L225LI)-expressing murine B cells that otherwise expand vigorously in vitro. However, although NF-κB is essential, previous work in mouse models has shown that enforced IKK signaling is not sufficient to induce lymphoma development. Although B cell-specific expression of a constitutively active allele of

IKKβ resulted in increased numbers of marginal zone B cells, the lifespan of such animals was not affected (15), a fundamental difference from the malignant phenotype induced by constitutive CBM signaling. Because Sasaki et al. (15) also used the CD19-Cre transgene to induce expression of the constitutively active (ca) IKKβ allele from a loxP-flanked STOP-modified ROSA26 locus, the genetic strategies for expressing CARD11(L225LI) or ca-IKKβ are identical. Thus, aberrant CBM signaling must trigger critical pathways, in addition to NF-κB, that drive oncogenesis. In line with this notion, we observed that mutated CARD11 triggers JNK activation in both primary murine B cells and human lymphoma lines. This finding is consistent with the known role of the physiological CBM complex in JNK activation during T-cell activation and further extends previous findings from retroviral gene transduction experiments showing that coiled-coil mutations in CARD11, which switch signals for self-antigen–induced cell death to T cell-independent proliferation, are also able to activate JNK (16, 34). Importantly, however, constitutive JNK activation was observed not only in transgenic B cells and manipulated lymphoma cells, but also at a high frequency in primary specimens from human ABC-DLBCL patients, highlighting the clinical relevance of our findings. Although it is unlikely that all these p-JNK–positive ABC-DLBCL cases would exhibit CARD11 mutations, multiple additional lymphomagenic alterations in DLBCL, and including activating lesions within the BCR signaling chains *Cd79a* or *-b,* channel their tumor-promoting activities through CARD11, BCL10, and MALT1 (13, 17). Those alterations are, therefore, also expected to engage the JNK pathway to drive tumorigenesis, which
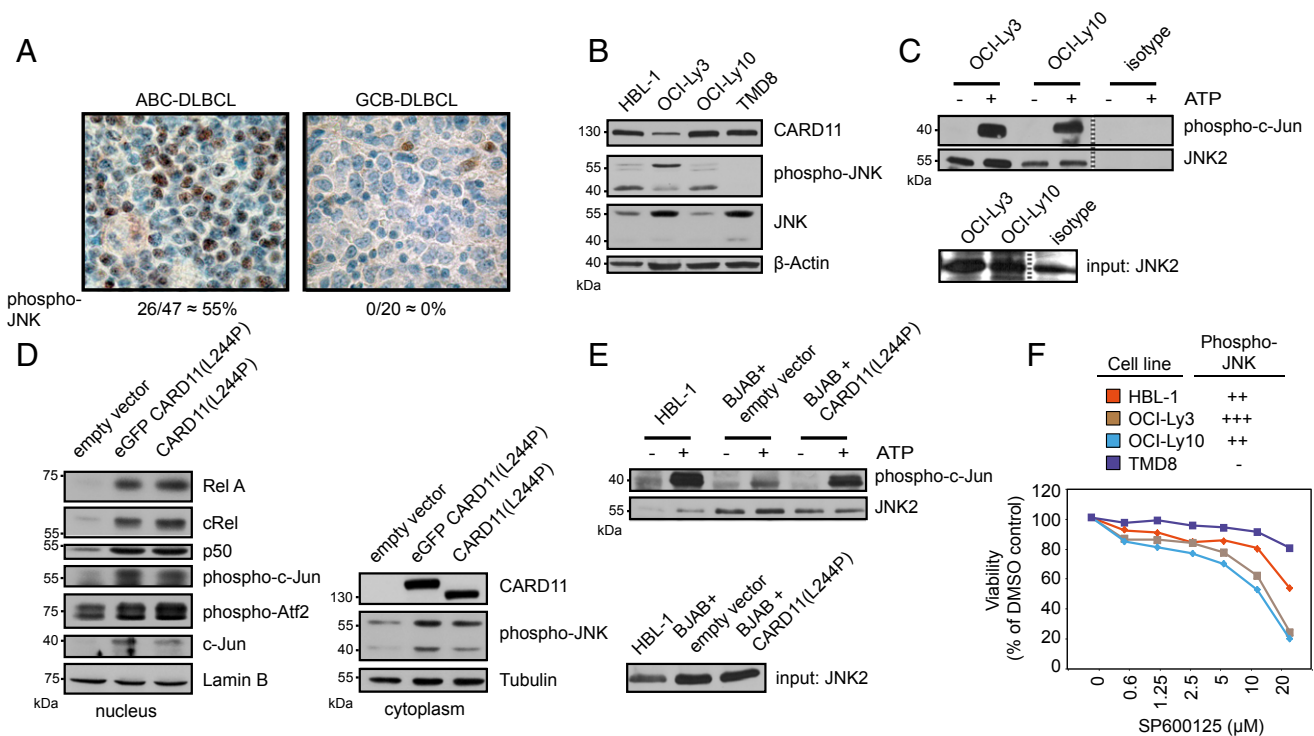
Fig. 6. JNK inhibition affects survival and proliferation of ABC-DLBCL cells. (*A*) Primary patient-derived ABC-DLBCL (*n* = 47) and GCB-DLBCL (*n* = 20) biopsy specimens were analyzed with phospho-JNK–specific antibodies. Representative data are shown; note internal positive controls in the otherwise phospho-JNK–negative GCB case. (Magnification, 400×.) (*B*) Immunoblots of different ABC-DLBCL cell lines. (*C*) JNK2 kinase assay performed with the ABC cell lines OCI-Ly3 and OCI-Ly10. (*D*) Non-ABC cell line BJAB was transduced with the empty vector, eGFP-tagged CARD11, harboring the OCI-Ly3 CARD11 mutation [CARD11 (L244P)] and CARD11(L244P) without the eGFP tag. The fractionated cell lysates were analyzed by immunoblotting. (*E*) A JNK2 kinase assay was performed with HBL-1 and BJAB cells expressing empty vector or CARD11(L244P). All experiments shown in *B–E* were performed twice. (*F*) Cell viability of different ABC-DLBCL cell lines after 48-h treatment with the JNK inhibitor SP600125. Representative results from six experiments are shown.

requires further study. In line with this hypothesis, a current study by Schmid et al. demonstrates that inactivations in DUSP4 can also induce constitutive JNK signaling in DLBCL (35).

Small molecule inhibition of JNK blocks autonomous growth of CARD11(L225LI)-expressing B cells, demonstrating that JNK activity is required for pathological CBM-induced B-lymphocyte proliferation. In human lymphoma cell lines, we also found that the specific ABC-DLBCL lines that exhibited aberrant JNK activity were also sensitive to JNK inhibitors, revealing a functionally important role for this pathway in human DLBCL. These findings are consistent with the cell survival role of JNK upon loss of DUSP4 in DLBCL (35), the known transformational potential of c-Jun (reviewed in refs. 18 and 36), and the aberrant activities of JNK and AP-1 signaling that are frequently observed in other human Hodgkin's and non-Hodgkin's lymphomas, in which they induce proliferation and suppress apoptosis (4, 37–41). How dysregulated CBM complexes couple mechanistically to the JNK pathway is still an open question. However, normal antigen receptor signaling recruits the kinase TAK1 to the CBM complex and thus initiates the AP-1 activation cascade (42), and BCL10 can act as a JNK-interacting protein that allows recruitment of JNK2 for c-Jun phosphorylation (43). In addition, the physiological assembly of CBM complexes induces proteolytic activity of the MALT1 paracaspase, which can cleave and inactivate the negative JNK regulator CYLD to enforce the signal for AP-1 activation (44-48). It is likely similar that those mechanisms would also be engaged by oncogenic CARD11 mutants, but this hypothesis remains to be investigated.

Because the current treatment options for DLBCL are limited and selective NF-κB inhibitors have failed clinical trials due to high toxicity, our results not only reveal previously unrecognized mechanistic insights into aberrant CBM function in vivo, but also

suggest that CBM downstream inhibition via JNK blockage with inhibitors such as SP600125 derivatives could constitute a therapeutic option for DLBCL patients with activated JNK signaling. Identification of the lymphocyte-specific mechanisms that couple dysregulated CBM activity to JNK could reveal additional strategies for inhibition of this pathway for lymphoma therapy.

Methods

Mice. The human *Card11L225LI* cDNA (13) was fused to an HA tag sequence preceded by a loxP-flanked transcriptional and translational STOP cassette and cloned into the ubiquitously expressed ROSA26 vector (15), which was linearized and electroporated into 129Ola ES cells. The clones were verified by Southern blot analysis with a 5′ flanking ROSA26 probe and specific PCR, as described (49). Blastocyst injection of the clones and subsequent chimera breeding resulted in CARD11(L225LI)^{stopFL} mice that were then crossed to CD19-Cre mice (16). The resulting bicistronic expression of CARD11(L225LI) together with eGFP allowed fluorescence monitoring of CARD11(L225LI)-expressing cells. The *BCL10*$^{-/-}$ and *MALT1*$^{-/-}$ alleles have been described previously (20, 21). Littermates were used in all subsequent experiments. All animal work was conducted in accordance with German Federal Animal Protection Laws and approved by the Institutional Animal Care and Use Committee at the Technische Universität München.

Cell Culture. The details of cell culture are provided in *SI Methods*.

Retroviral Transductions. The details of retroviral transductions are provided in *SI Methods*.

B-Cell Purification. The details of B-cell purifications are provided in *SI Methods*.

Gel Mobility Shift Assays and Western Blotting. Cytosolic and nuclear extracts were obtained using standard methods (18), and protein concentrations were determined by the Bradford assay. A 5-μg sample of nuclear extract

was incubated with IRDye700-labeled, double-stranded oligonucleotide probes for NF-κB or AP-1, and the gels were analyzed using the Odyssey Infrared Imaging System (Licor Biosciences), as previously described (18). Western blots were probed using antibodies against the following proteins: CARD11 (1D12), no. 4435; p50, no. 3035; BCL10 (C78F1), no. 4237; phospho-IκBα, no. 9241; IκBα, no. 9242; p-c-Jun, no. 8794; phospho-JNK, no. 9251; JNK, no. 9252; phospho-Atf2, no. 5112; phospho-SYK, no. 2715; phospho-AKT, no. 9275; phospho-ERK, no. 4370 (all obtained from Cell Signaling Technology); β-actin, no. 5060 (Sigma); HA high affinity (3F10) (Roche); RelA, no. sc-372; tubulin (B-7), no. sc-5286; lamin B (M-20), no. sc-6217; cRel, no. sc-71; CK1α, no. sc6477; c-Jun, no. sc-1694 (all from Santa Cruz Biotechnology); and MALT1 (Genentech).

Flow Cytometry. Tissues were processed into single-cell suspensions and treated with red blood cell lysis buffer, and cells were transferred into PBS containing 3% FBS. After incubation with Fc-block (CD16/32), the cells were stained for 30 min at 4 °C, washed, and analyzed using a FACSCanto II Flow Cytometer (BD) and FlowJo software (Tree Star, Inc.). The following antibodies were used: B220 (RA3-6B2), TCR-β (H57-597), CD80 (16-1QA1), CD86 (GL1), IgM (II/41), CD19 (1D3), CD21 (4E3), MHCII (M5/114.15.2), CD25 (PC61.5), Sca-1 (D7), CD43 (eBioR2/60), CXCR4 (2B11), IL-7R (A7R34) (all eBioscience); and CD138 (281-2) and Igκ (187.1) (from BD).

Measurement of Serum Cytokine and Ig Levels. The details of serum cytokine and Ig level measurements are provided in *SI Methods*.

RNA and quantitative RT-PCR. The details of RNA and quantitative (q)RT-PCR are provided in *SI Methods*.

Inhibitor Treatment. CARD11(L225LI)$^{CD19-Cre}$ splenocytes were grown in RPMI-1640 medium supplemented with 10% (vol/vol) FBS containing 2 mM L-glutamine and 0.1% β-mercaptoethanol. Bay11-7082, SP600125, and PD98,059 were obtained from Sigma-Aldrich. Cal-101 and PCI-32765 were purchased from SelleckChem. R406 was purchased from ICS International Clinical Service GmbH. The inhibitors were dissolved in DMSO and used at the indicated concentrations. Cell viability was quantified by flow cytometry with Annexin V and 7-AAD staining (eBioscience).

Cell Viability Assay. Human DLBCL cells were seeded in 96-well round-bottom plates at a concentration of 5×10^4 cells per mL and treated with serial dilutions of the JNK inhibitor SP600125 or DMSO as a solvent control at concentrations between 20 μM and 0.3 μM. After incubation for 48 h, cell viability was determined using the CellTiter-Glo Luminescent Cell Viability Assay (Promega) according to the manufacturer's protocol. Cell treatment and viability analyses were performed in duplicate.

Nonradioactive JNK2 Kinase Assay. The details of the nonradioactive JNK2 kinase assay are provided in *SI Methods*.

Histology. Mouse organs were fixed in 4% (vol/vol) formaldehyde and paraffin-embedded. Sections were stained with hematoxylin and eosin (H&E) and Ki-67 (SP6; Thermo Fisher Scientific) using an automated immunostainer (Leica Bond III) according to the manufacturer's protocol. The immunoperoxidase stain was performed on an automated immunostainer (Benchmark; Ventana/Roche). Primary antibody dilution pJNK no. 4668 (Cell Signaling Technology) was used 1:50. Antigen retrieval was achieved by cell conditioning (CC1; Ventana/Roche) treatment for 92 min.

Statistical Analysis. Where indicated, the results were analyzed for statistical significance using an unpaired two-tailed Student's t test: *** statistically significant ($P < 0.0001$); **$P < 0.01$; *$P < 0.05$; ns, not statistically significant ($P \geq 0.05$). The differences between groups were considered significant at P values of <0.05. The differences in animal survival (Kaplan–Meier survival curves) were analyzed by a log-rank test.

1. Lenz G, Staudt LM (2010) Aggressive lymphomas. *N Engl J Med* 362(15):1417–1429.
2. Lenz G, et al.; Lymphoma/Leukemia Molecular Profiling Project (2008) Stromal gene signatures in large-B-cell lymphomas. *N Engl J Med* 359(22):2313–2323.
3. Alizadeh AA, et al. (2000) Distinct types of diffuse large B-cell lymphoma identified by gene expression profiling. *Nature* 403(6769):503–511.
4. Staudt LM (2010) Oncogenic activation of NF-kappaB. *Cold Spring Harb Perspect Biol* 2(6):a000109.
5. Lam LT, et al. (2005) Small molecule inhibitors of IkappaB kinase are selectively toxic for subgroups of diffuse large B-cell lymphoma defined by gene expression profiling. *Clin Cancer Res* 11(1):28–40.
6. Olsen LS, et al. (2004) Anticancer agent CHS 828 suppresses nuclear factor-kappa B activity in cancer cells through downregulation of IKK activity. *Int J Cancer* 111(2): 198–205.
7. Ravaud A, et al. (2005) Phase I study and pharmacokinetic of CHS-828, a guanidino-containing compound, administered orally as a single dose every 3 weeks in solid tumours: An ECSG/EORTC study. *Eur J Cancer* 41(5):702–707.
8. Dal Porto JM, et al. (2004) B cell antigen receptor signaling 101. *Mol Immunol* 41(6-7): 599–613.
9. Sommer K, et al. (2005) Phosphorylation of the CARMA1 linker controls NF-kappaB activation. *Immunity* 23(6):561–574.
10. Shinohara H, et al. (2005) PKC beta regulates BCR-mediated IKK activation by facilitating the interaction between TAK1 and CARMA1. *J Exp Med* 202(10):1423–1431.
11. Shinohara H, Kurosaki T (2009) Comprehending the complex connection between PKCbeta, TAK1, and IKK in BCR signaling. *Immunol Rev* 232(1):300–318.
12. Ngo VN, et al. (2006) A loss-of-function RNA interference screen for molecular targets in cancer. *Nature* 441(7089):106–110.
13. Lenz G, et al. (2008) Oncogenic CARD11 mutations in human diffuse large B cell lymphoma. *Science* 319(5870):1676–1679.
14. Lamason RL, McCully RR, Lew SM, Pomerantz JL (2010) Oncogenic CARD11 mutations induce hyperactive signaling by disrupting autoinhibition by the PKC-responsive inhibitory domain. *Biochemistry* 49(38):8240–8250.
15. Sasaki Y, et al. (2006) Canonical NF-kappaB activity, dispensable for B cell development, replaces BAFF-receptor signals and promotes B cell proliferation upon activation. *Immunity* 24(6):729–739.
16. Rickert RC, Roes J, Rajewsky K (1997) B lymphocyte-specific, Cre-mediated mutagenesis in mice. *Nucleic Acids Res* 25(6):1317–1318.
17. Shapiro-Shelef M, Calame K (2005) Regulation of plasma-cell development. *Nat Rev Immunol* 5(3):230–242.
18. Ferch U, et al. (2009) Inhibition of MALT1 protease activity is selectively toxic for activated B cell-like diffuse large B cell lymphoma cells. *J Exp Med* 206(11):2313–2320.
19. Bidère N, et al. (2009) Casein kinase 1α governs antigen-receptor-induced NF-κB activation and human lymphoma cell survival. *Nature* 458(7234):92–96.
20. Ruland J, et al. (2001) Bcl10 is a positive regulator of antigen receptor-induced activation of NF-kappaB and neural tube closure. *Cell* 104(1):33–42.
21. Ruland J, Duncan GS, Wakeham A, Mak TW (2003) Differential requirement for Malt1 in T and B cell antigen receptor signaling. *Immunity* 19(5):749–758.
22. Hara H, et al. (2003) The MAGUK family protein CARD11 is essential for lymphocyte activation. *Immunity* 18(6):763–775.
23. Musti AM, Treier M, Bohmann D (1997) Reduced ubiquitin-dependent degradation of c-Jun after phosphorylation by MAP kinases. *Science* 275(5298):400–402.
24. Gupta S, Campbell D, Dérijard B, Davis RJ (1995) Transcription factor ATF2 regulation by the JNK signal transduction pathway. *Science* 267(5196):389–393.
25. Keller SA, Schattner EJ, Cesarman E (2000) Inhibition of NF-kappaB induces apoptosis of KSHV-infected primary effusion lymphoma cells. *Blood* 96(7):2537–2542.
26. Bennett BL, et al. (2001) SP600125, an anthrapyrazolone inhibitor of Jun N-terminal kinase. *Proc Natl Acad Sci USA* 98(24):13681–13686.
27. Shi-Wen X, et al. (2006) Constitutive ALK5-independent c-Jun N-terminal kinase activation contributes to endothelin-1 overexpression in pulmonary fibrosis: Evidence of an autocrine endothelin loop operating through the endothelin A and B receptors. *Mol Cell Biol* 26(14):5518–5527.
28. Plantevin Krenitsky V, et al. (2012) Discovery of CC-930, an orally active anti-fibrotic JNK inhibitor. *Bioorg Med Chem Lett* 22(3):1433–1438.
29. Friedberg JW, et al. (2010) Inhibition of Syk with fostamatinib disodium has significant clinical activity in non-Hodgkin lymphoma and chronic lymphocytic leukemia. *Blood* 115(13):2578–2585.
30. Brown JR (2013) Ibrutinib (PCI-32765), the first BTK (Bruton's tyrosine kinase) inhibitor in clinical trials. *Curr Hematol Malig Rep* 8(1):1–6.
31. Meyer PN, et al. (2011) Immunohistochemical methods for predicting cell of origin and survival in patients with diffuse large B-cell lymphoma treated with rituximab. *J Clin Oncol* 29(2):200–207.
32. Wilson WH, et al. (2015) Targeting B cell receptor signaling with ibrutinib in diffuse large B cell lymphoma. *Nat Med* 21(8):922–926.
33. Davis RE, et al. (2010) Chronic active B-cell-receptor signalling in diffuse large B-cell lymphoma. *Nature* 463(7277):88–92.
34. Jeelall YS, et al. (2012) Human lymphoma mutations reveal CARD11 as the switch between self-antigen-induced B cell death or proliferation and autoantibody production. *J Exp Med* 209(11):1907–1917.
35. Schmid CA, et al. (2015) DUSP4 deficiency caused by promoter hypermethylation drives JNK signaling and tumor cell survival in diffuse large B cell lymphoma. *J Exp Med* 212(5):775–792.
36. Jochum W, Passegué E, Wagner EF (2001) AP-1 in mouse development and tumorigenesis. *Oncogene* 20(19):2401–2412.
37. Hess P, Pihan G, Sawyers CL, Flavell RA, Davis RJ (2002) Survival signaling mediated by c-Jun NH(2)-terminal kinase in transformed B lymphoblasts. *Nat Genet* 32(1):201–205.

38. Mathas S, et al. (2002) Aberrantly expressed c-Jun and JunB are a hallmark of Hodgkin lymphoma cells, stimulate proliferation and synergize with NF-kappa B. *EMBO J* 21(15):4104–4113.

39. Wang M, et al. (2009) JNK is constitutively active in mantle cell lymphoma: Cell cycle deregulation and polyploidy by JNK inhibitor SP600125. *J Pathol* 218(1):95–103.

40. Trøen G, et al. (2004) Constitutive expression of the AP-1 transcription factors c-jun, junD, junB, and c-fos and the marginal zone B-cell transcription factor Notch2 in splenic marginal zone lymphoma. *J Mol Diagn* 6(4):297–307.

41. Leventaki V, et al. (2014) c-JUN N-terminal kinase (JNK) is activated and contributes to tumor cell proliferation in classical Hodgkin lymphoma. *Hum Pathol* 45(3):565–572.

42. Shim JH, et al. (2005) TAK1, but not TAB1 or TAB2, plays an essential role in multiple signaling pathways in vivo. *Genes Dev* 19(22):2668–2681.

43. Blonska M, et al. (2007) The CARMA1-Bcl10 signaling complex selectively regulates JNK2 kinase in the T cell receptor-signaling pathway. *Immunity* 26(1):55–66.

44. Coornaert B, et al. (2008) T cell antigen receptor stimulation induces MALT1 paracaspase-mediated cleavage of the NF-kappaB inhibitor A20. *Nat Immunol* 9(3):263–271.

45. Rebeaud F, et al. (2008) The proteolytic activity of the paracaspase MALT1 is key in T cell activation. *Nat Immunol* 9(3):272–281.

46. Staal J, et al. (2011) T-cell receptor-induced JNK activation requires proteolytic in-activation of CYLD by MALT1. *EMBO J* 30(9):1742–1752.

47. Uehata T, et al. (2013) Malt1-induced cleavage of regnase-1 in CD4(+) helper T cells regulates immune activation. *Cell* 153(5):1036–1049.

48. Gewies A, et al. (2014) Uncoupling Malt1 threshold function from paracaspase activity results in destructive autoimmune inflammation. *Cell Reports* 9(4):1292–1305.

49. Pechloff K, et al. (2010) The fusion kinase ITK-SYK mimics a T cell receptor signal and drives oncogenesis in conditional mouse models of peripheral T cell lymphoma. *J Exp Med* 207(5):1031–1044.